Ersch. in: Proceedings of the National Academy of Sciences of the United States of America ; 102 (2005), 36. - S. 12653-12655

http://dx.doi.org/10.1073/pnas.0502577102

# Amorphous layer around aragonite platelets in nacre

**Nadine Nassif*†, Nicola Pinna‡§, Nicole Gehrke*, Markus Antonietti*, Christian Jäger¶, and Helmut Cölfen*†**

*Colloid Chemistry Department, Max Planck Institute of Colloids and Interfaces, Research Campus Golm, D-14424 Potsdam, Germany; ‡Institut für Anorganische Chemie, Martin-Luther-Universität Halle-Wittenberg, Kurt-Mothes-Strasse 2, 06120 Halle (Saale), Germany; §Max Planck Institute of Microstructure Physics, Weinberg 2, D-06120 Halle (Saale), Germany; and ¶Division I.3, Federal Institute for Materials Research and Testing, Richard Willstaetter Strasse 11, D-12489 Berlin, Germany

**We reveal that the aragonite $CaCO_3$ platelets in nacre of *Haliotis laevigata* are covered with a continuous layer of disordered amorphous $CaCO_3$ and that there is no protein interaction with this layer. This finding contradicts classical paradigms of biomineralization, e.g., an epitaxial match between the structural organic matrix and the formed mineral. This finding also highlights the role of physicochemical effects in morphogenesis, complementing the previously assumed total control by biomolecules and bioprocesses, with many implications in nanotechnology and materials science.**

amorphous calcium carbonate | biomineralization | high-resolution transmission EM | solid-state NMR

The delicate mineral structures produced by organisms in the process of biomineralization are widely recognized as inspiration for future materials science and nanotechnology because of their unique materials properties and their hierarchical order often over several length scales (1). Therefore, recent multidisciplinary research has focused on understanding biomineralization processes and exploring ways to mimic them (1). Particularly well investigated is nacre, possessing a 3,000-fold enhanced fracture resistance compared with pure aragonite, with implications on building material design. Nacre is composed of aragonite platelets, a usually metastable $CaCO_3$ polymorph, with [001] orientation toward protein-covered $\beta$-chitin layers (2).

The present paradigm discusses an epitaxial match of acidic proteins adsorbed on the insoluble matrix with the atomic structure of the aragonite (001) plane (3). Indeed, two independent studies reported aragonite formation in the presence of soluble proteins extracted from a nacreous aragonite biomineral layer (4, 5). However, because the extracted macromolecules are disordered species and mixtures, too (5), an epitaxial match seems questionable. We therefore revisited nacre aragonite single crystalline platelets from the abalone *Haliotis laevigata* (6) with high-resolution transmission electron microscopy (HRTEM) supplemented by solid-state $^{13}C$ and $^{1}H$ NMR to obtain information on the organic–inorganic interface.

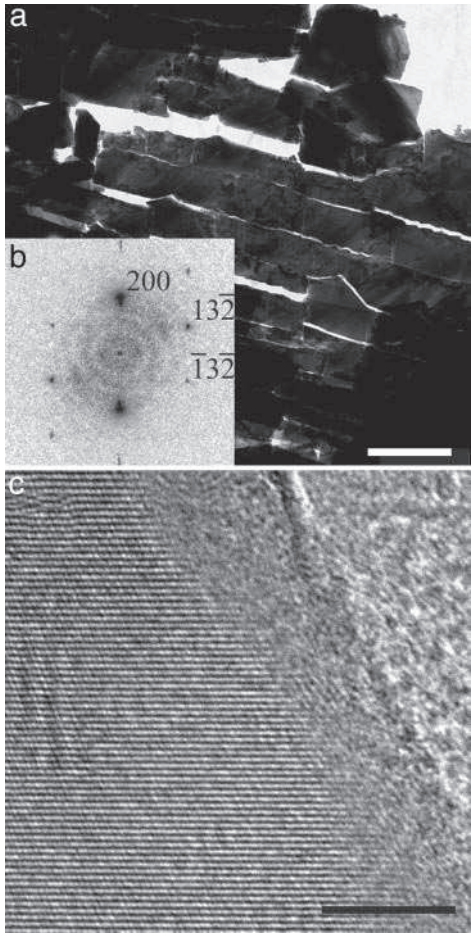


**Fig. 1.** TEM study of nacre platelets. (*a*) TEM micrograph of a TEM thin cut of the aragonite platelets in nacre. (Scale bar: 1 $\mu$m.) (*b*) Power spectrum of the HRTEM micrograph in *c*. The crystal is oriented along the [023] direction. (*c*) HRTEM micrograph of a selected surface area of the single crystalline aragonite platelets. (Scale bar: 5 nm.)

## Materials and Methods

Nacre was obtained from the shell of the abalone *H. laevigata*, which belongs to the gastropoda. The structure of the nacreous layer is described in refs. 6–8. Thin cuts from the nacreous part were made with a diamond knife in a Leica ultracut UCT and transferred onto an amorphous carbon-coated copper grid. By using this technique, artifacts in the form of amorphous regions in the sample as can be observed by the ion milling technique (9) can be avoided. A Philips CM200 FEG transmission electron microscope, operating at 200 kV, equipped with a field emission gun was used. Alternatively, a JEOL 4010 operated at 400 kV equipped with a $LaB_6$ cathode was applied. The NMR experiments have been carried out by using an AVANCE 600 spectrometer (Bruker, Billerica, MA) using a double-resonant 7-mm probe at sample rotation magic angle spinning (MAS) frequencies of 6.5 kHz. $^{1}H$ MAS NMR spectra have been acquired with repetition times of 2 s up to 25 s and typically 64 scans. $^{13}C$ MAS NMR spectra required repetition times of 40 min, and 44 scans were accumulated. For the $^{1}H\{^{13}C\}$ cross-polarization (CP) measurements, up to 16 k scans (1 k = 1,024) were collected with CP times of 1 and 8 ms and dipolar decoupling and repetition times of 2 and 6 s. Two-dimensional heteronuclear correlation experiments were conducted by using CP times of 1 and 8 ms, 48 $t_1$ increments spaced by 5 $\mu$s (200 kHz frequency range in the $^{1}H$ dimension, States mode), and a total of 1 k scans per increment.

Abbreviations: ACC, amorphous $CaCO_3$; CP, cross-polarization; HRTEM, high-resolution transmission EM; MAS, magic angle spinning.

†To whom correspondence may be addressed. E-mail: coelfen@mpikg.mpg.de or nadine.nassif@mpikg.mpg.de.



Konstanzer Online-Publikations-System (KOPS)
URL: http://nbn-resolving.de/urn:nbn:de:bsz:352-166471

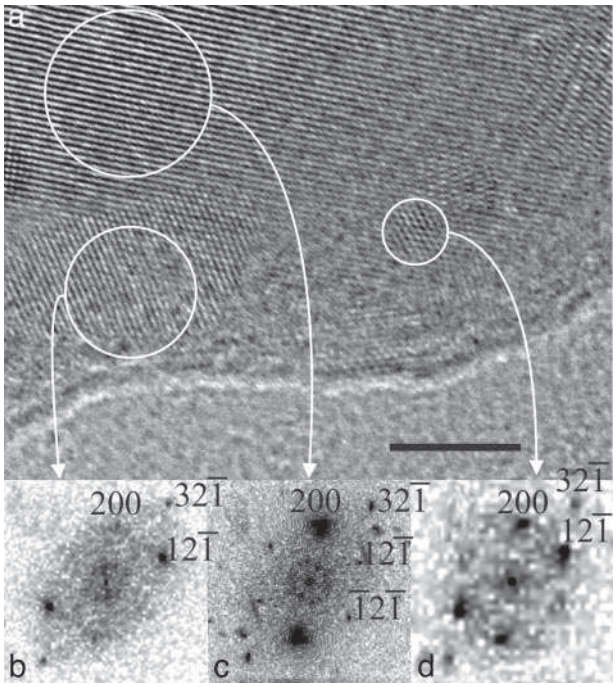


**Fig. 2.** HRTEM study of beam-damaged nacre platelets. (*a*) HRTEM micrograph of a selected surface area of the single crystalline aragonite platelets after irradiation. (Scale bar: 5 nm.) (*b* and *d*) Power spectra of the crystallized ACC layer. (*c*) Power spectrum of the core of the platelet. The crystal is oriented along the [012] direction.

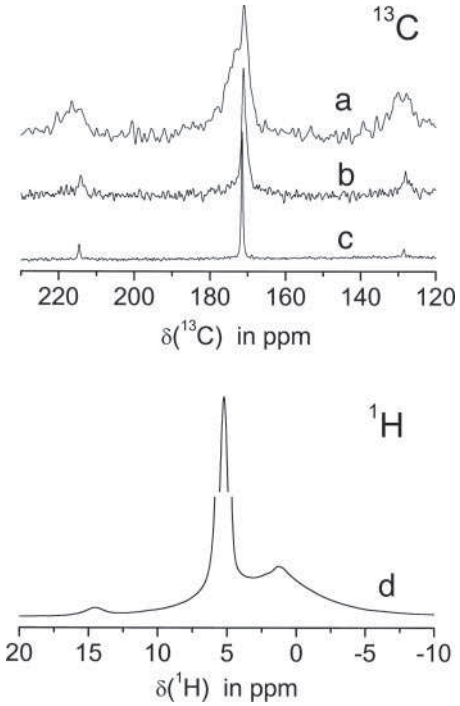


**Fig. 3.** NMR spectra of nacre. (*Upper*) $^{13}$C NMR spectra of the carboxyl region also displaying the spinning sidebands. Trace a, CP MAS spectrum of the protein (CP time: 1 ms); trace b, CP MAS spectrum of the amorphous carbonate (CP time: 8 ms) in comparison with the single pulse experiment; trace c, showing the aragonite resonance of the crystals. (*Lower*) Trace d shows the $^{1}$H spectrum at 12.5 kHz. Note the interception of the *y* axis between 25% and 75% of the water signal at 5.8 ppm to display the weak line at 14.4 ppm.

## Results

When observing microtomed nacre thin cuts (Fig. 1*a*) with HRTEM, surprisingly, in all cases a 3- to 5-nm amorphous $CaCO_3$ (ACC) layer was detected as a continuous coating of single crystalline aragonite (Fig. 1 *b* and *c*), which was never previously reported in the numerous studies of nacre. Although ACC is discussed as a building material in biomineralization (10), the detected continuous external ACC coating is contradicting the epitaxy paradigm (3).

The amorphous character of the ACC layer was proven by visible crystallization under intense electron irradiation, also excluding an organic nature of this layer. Fig. 2*a* and Fig. 4, which is published as supporting information on the PNAS web site, present a HRTEM image of an edge of a platelet after electron irradiation. The aragonite platelet is oriented along the [012] direction as demonstrated by its power spectrum (Fig. 2*c*). Surprisingly, at its edge the ACC layer starts to crystallize, forming several crystalline nuclei. Their structural characterization reveals that they are indeed made of aragonite that is slightly distorted compared with the aragonite of the core of the platelet (Fig. 2 *b* and *d*). Kinetic studies of the crystallization behavior under electron irradiation from same zone are shown in Fig. 4. It can be observed that little clusters in the amorphous layer start to crystallize (black circles) during the irradiation (the irradiation time increases from *a* to *c*).

The $^{1}$H{$^{13}$C} CP NMR spectrum taken with 1-ms CP time clearly reveals the presence of the protein matrix. In Fig. 3*a*, the carboxyl region at ≈180 ppm is shown with the spinning sidebands of these lines symmetrically around it. Simply by changing the CP time to 8 ms, these protein signals can be suppressed almost completely, and the NMR signal of a distorted carbonate group appears (Fig. 3*b*). That this group is distorted (amorphous character) can readily be seen by comparison with the much narrower $^{13}$C lineshape of the aragonite crystals (Fig. 3*c*). The structure of the spinning sidebands definitely proves that this is a carbonate group.

Furthermore, 2D heteronuclear experiments (data not shown) verify that two different proton species cross-polarize those disordered carbonate groups: water with a chemical shift of 5.5 ppm (Fig. 3*d*, strong signal) and, additionally, the protons causing the very weak 14.4 ppm signal. Although the structural nature of this proton signal is not yet known, it can be ruled out that it belongs to the protein matrix. In that case, one should observe a similarly narrow correlation signal to the aliphatic region, which is not observed here.

## Discussion

The detected disordered ACC coating of the single crystalline aragonite platelets is clear evidence against an epitaxial match between the organic matrix and the formed aragonite (3). In addition, both material interfaces (aragonite/ACC as well as ACC/matrix) are significantly undulated in every sample and cut direction, also opposing the classical picture of biomineral growth. The coarsed interface suggests that nacre is built by mesoscale transformation (11) from amorphous colloidal intermediates (10, 11). Further support against the epitaxial match is given by solid-state NMR (these NMR results will be published in detail elsewhere). Summarizing all NMR data, it can be concluded that there is a disordered carbonate group that can be cross-polarized by two different protons, which is not the case for the aragonite carbonate group. These disordered surface carbonate sites obviously are not bound to protein. It is suggested that because of the present disorder these sites are located at the crystal surfaces.

ACC is known as inherently unstable in an aqueous environment, but the present ACC layer almost perfectly coats a

metastable $CaCO_3$ polymorph. One possible explanation for this layer is the exclusion of impurities and expelled macromolecules from the single crystalline aragonite layer throughout crystallization, similar to the zone-melting process in metallurgy. The result is aragonite with an ACC coating kinetically stabilized by ''impurities,'' which would destabilize a crystal lattice and thus prevent crystallization. A second, presumably cooperating option is the role of interface energy: the unusual [001] orientation of aragonite platelets exposes large areas of high-energy crystal faces. Much energy can be gained by surface reconstitution toward an amorphous gradient surface layer: one costly interface is substituted by two with much lower energy. The amorphous coating and binding layer also could provide better adhesion and mechanical performance of the hybrid material, similar to interface polymers in natural polymeric composites (12).

Our results are not in contradiction to the observed [001] orientation of the aragonite platelets within the organic matrix. If aragonite is nucleated, the (001) face is part of the default morphology. According to the Debye–Hückel theory for slab geometries (13), the charge interaction of the highly polar aragonite (001) face can extend throughout the 3- to 5-nm ACC layer with a contribution of up to $\approx$0.04 kT per charge (13). For $>$25 charges on the (001) face, the thermal particle motion will already be overcome, and the particle can stick to an oppositely charged organic matrix with [001] orientation so that the simple presence of charge could already be a possible explanation for the crystal alignment.

In summary, the observation of amorphous top layers in biominerals shows a previously unrecognized, exciting way to address interface binding without the need for epitaxial relations between soft and hard matter and also highlights the usually neglected role of physicochemical effects in such processes.

We thank the Fritz-Haber Institute and Prof. R. Schlögl for use of the HRTEM electron microscope and Klaus Weiss for his technical assistance. We also thank Dr. habil. M. Fritz (University of Bremen, Bremen, Germany) for the nacre samples. This work was supported by the Deutsche Forschungsgemeinschaft within the priority program ''Principles of Biomineralization'' and by the Max Planck Society.

1. Mann, S. (2001) *Biomineralization, Principles and Concepts in Bioinorganic Materials Chemistry* (Oxford Univ. Press, New York).
2. Lowenstam, H. A. & Weiner, S. (1989) *On Biomineralization* (Oxford Univ. Press, New York).
3. Weiner, S. & Traub, W. (1980) *FEBS Lett.* **111,** 311–316.
4. Falini, G., Albeck, S., Weiner, S. & Addadi, L. (1996) *Science* **271,** 67–69.
5. Belcher, A. M., Wu, X. H., Christensen, R. J., Hansma, P. K., Stucky, G. D. & Morse, D. E. (1996) *Nature* **381,** 56–58.
6. Weiss, I. M., Kaufmann, S., Mann, K. & Fritz, M. (2000) *Biochem. Biophys. Res. Commun.* **267,** 17–21.
7. Wise, S. W. (1970) *Science* **167,** 1486–1488.
8. Nakahara, H., Bevelander, G. & Kakei, M. (1981) *Venus* **41,** 33–46.
9. Rousseau, M., Lopez, E., Stempfle, P., Brendle, M., Franke, L., Guette, A., Naslain, R. & Bourrat, X. (2005) *Biomaterials* **26,** 6254–6262.
10. Politi, Y., Arad, T., Klein, E., Weiner, S. & Addadi, L. (2004) *Science* **306,** 1161–1164.
11. Cölfen, H. & Mann, S. (2003) *Angew. Chem. Int. Ed.* **42,** 2350–2365.
12. Fratzl, P., Burgert, I. & Gupta, H. S. (2004) *Phys. Chem. Chem. Phys.* **6,** 5575–5579.
13. Netz, R. R. (2000) *Eur. Phys. J. E* **3,** 131–141.